**ISCI, Volume *16***

## Supplemental Information

# High-Performance Planar Perovskite Solar Cells with Negligible Hysteresis Using 2,2,2-Trifluoroethanol-Incorporated $SnO_2$

**Yigang Luan, Xiaohui Yi, Peng Mao, Yuanzhi Wei, Jing Zhuang, Ningli Chen, Tao Lin, Cheng Li, and Jizheng Wang**

## Supplemental Information

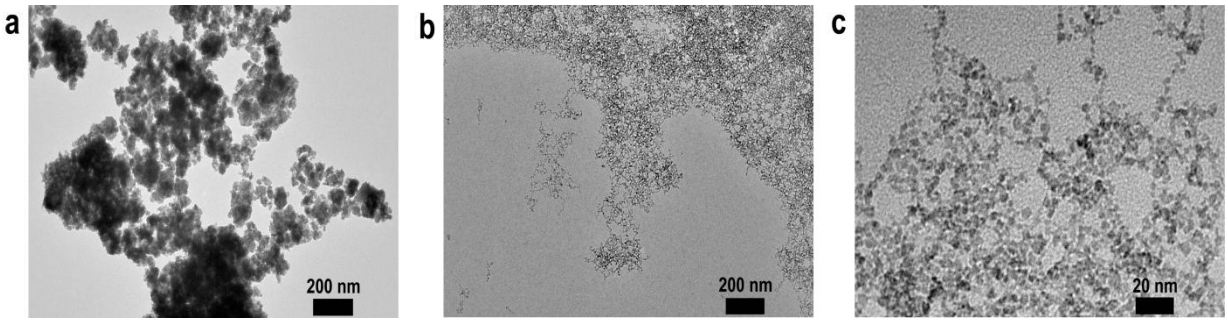


**Figure S1** TEM images of the a) $SnO_2$ and b,c) T-$SnO_2$ nanoparticles. Related to figure 1.

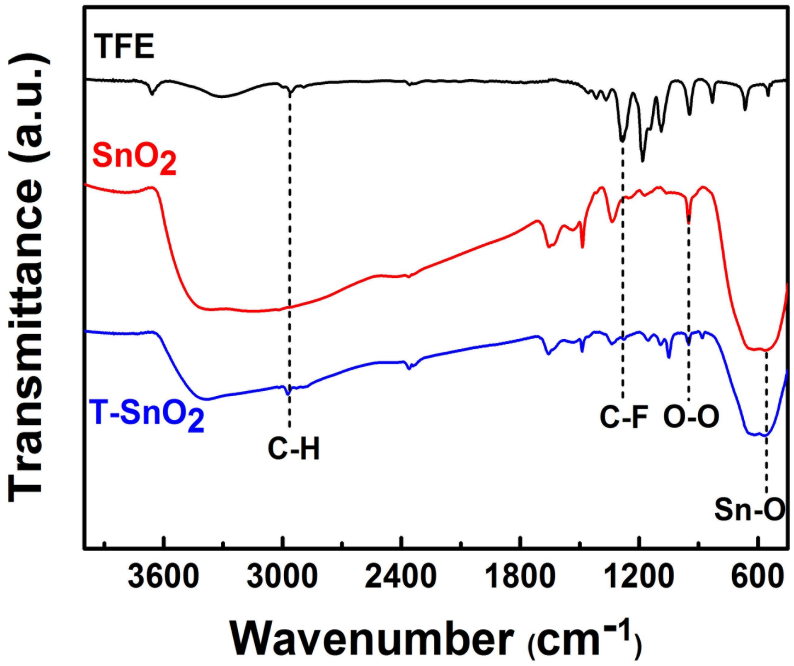


**Figure S2** FTIR spectra of the TFE, $SnO_2$ and T-$SnO_2$ films. Related to figure 1A and 1B.

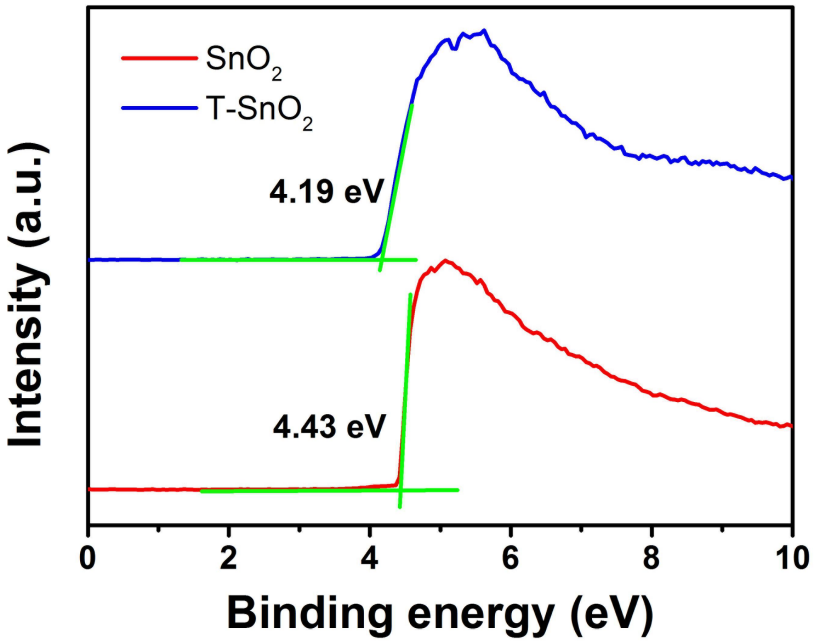


**Figure S3** The UPS cut-off edge of the $SnO_2$ and T-$SnO_2$ films. Relate to figure 1D.

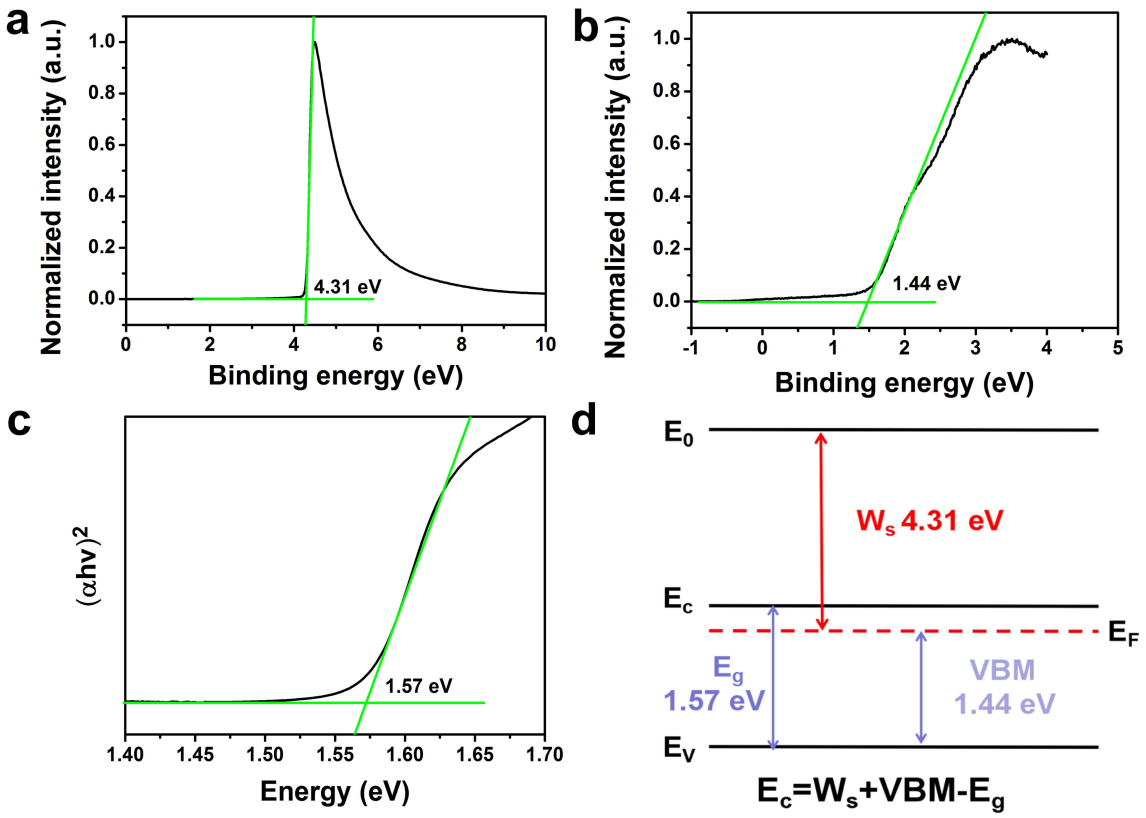


**Figure S4** The UPS data of the perovskite film. a) the cut-off edge. b) Valence band. c) Bandgap. d) band structure. It can be calculated that the conduction band ($E_c$) of the perovskite is 4.18 eV. Relate to figure 1D.

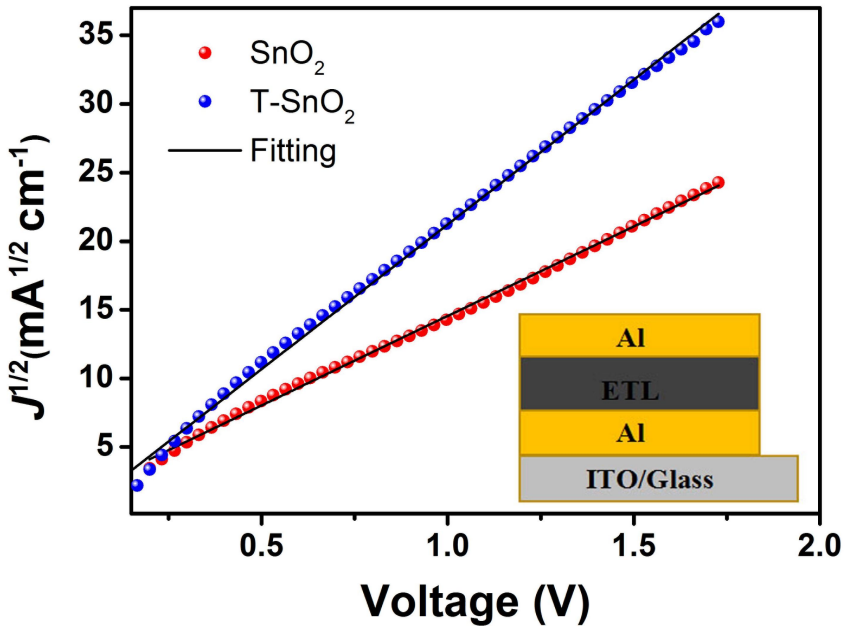


**Figure S5** The electron mobility for the $SnO_2$ and T-$SnO_2$ films calculated by the SCLC model with the device structure of Glass/ITO/Al/ETL/Al. Related to figure 1.

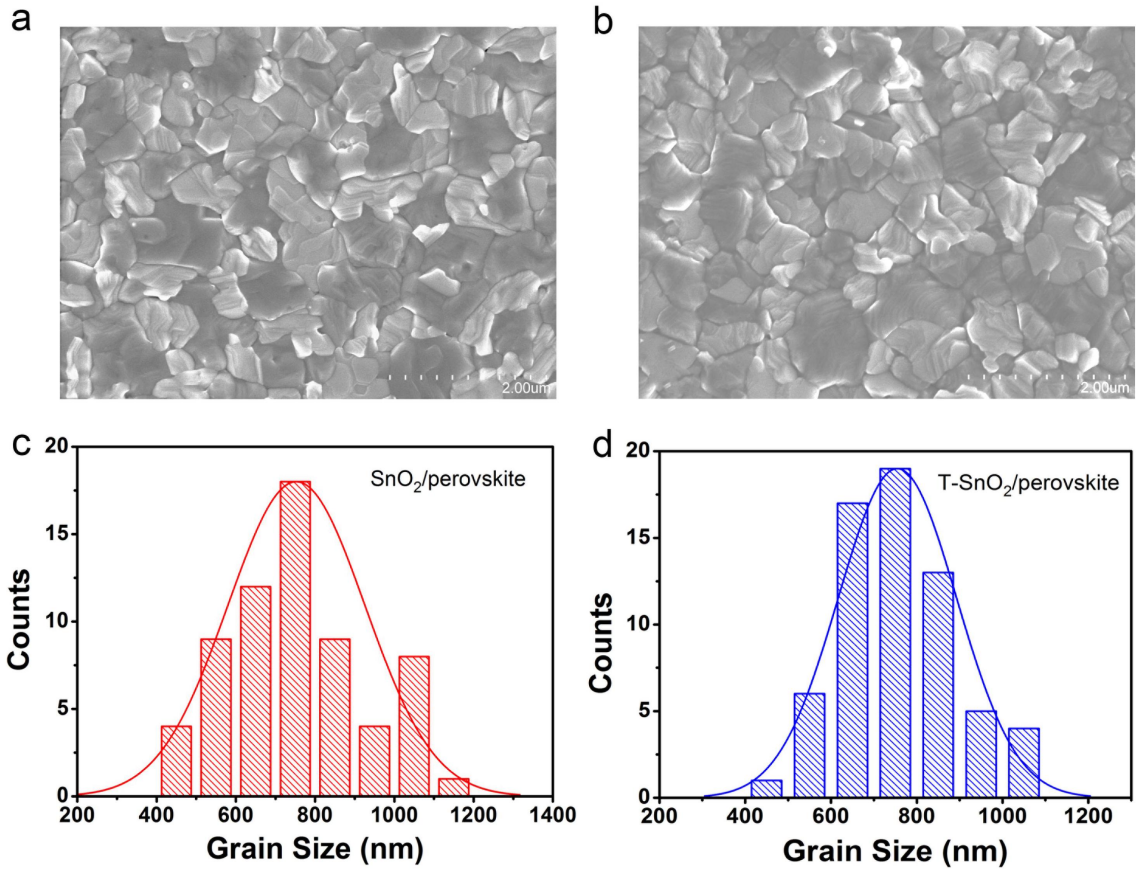


**Figure** S6 The morphology of perovskite deposited on the $SnO_2$ and T-$SnO_2$ substrates. Top-view SEM images and the grain size distribution of perovskite coated on a,c) $SnO_2$ and b,d) T-$SnO_2$. Related to figure 2.

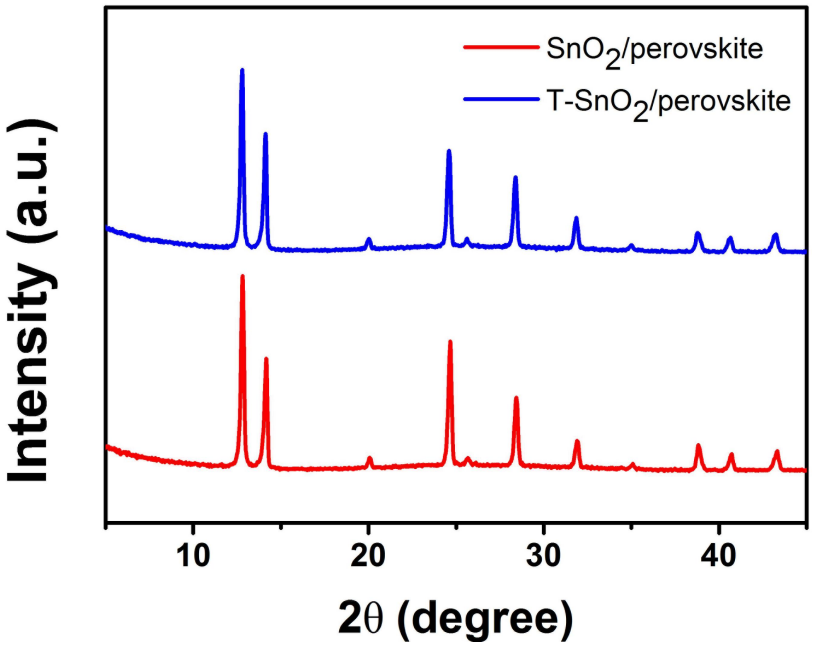


**Figure S7** XRD spectra of the perovskite film grown on the $SnO_2$ and T-$SnO_2$ ETLs. Related to figure 2.

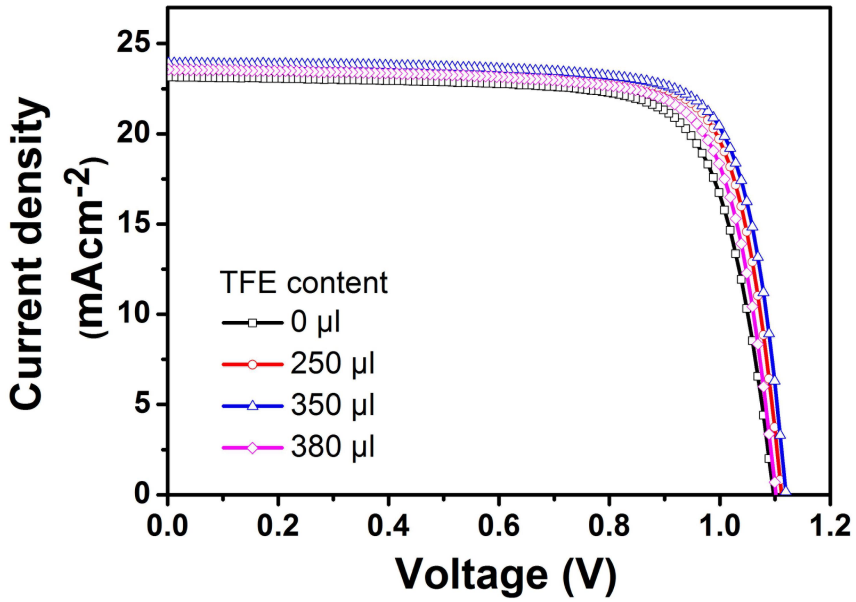


**Figure S8** *J-V* curves of the PSCs based on the T-$SnO_2$ ETLs. T-$SnO_2$ ETLs with various TFE contents in the $SnO_2$ solution. The solar cells show the optimum performance at the TFE volume of 350 µl. Related to figure 2B.

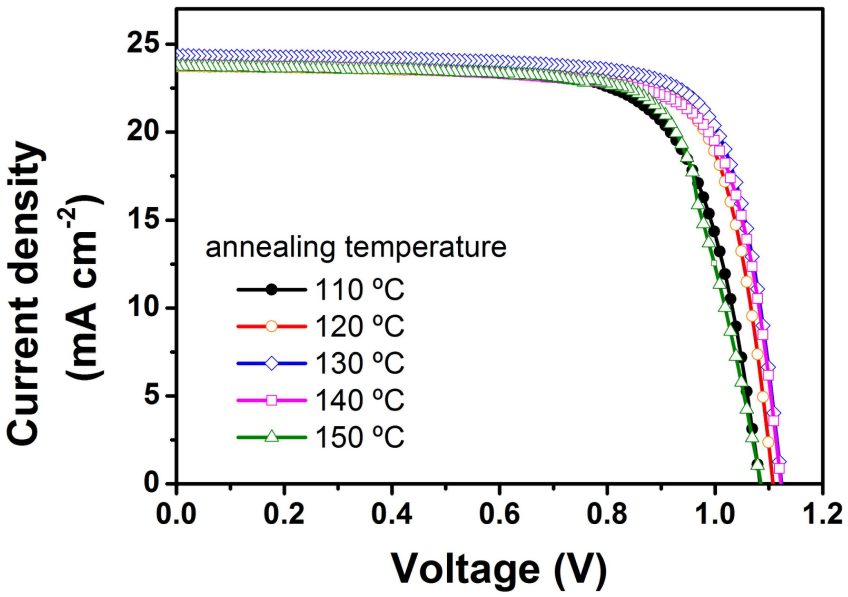


**Figure S9** *J-V* curves of the PSCs based on the T-$SnO_2$ ETLs. T-$SnO_2$ ETLs with various annealing temperatures. The solar cells show the best performance at the annealing temperature of 130°C. Related to figure 2B.

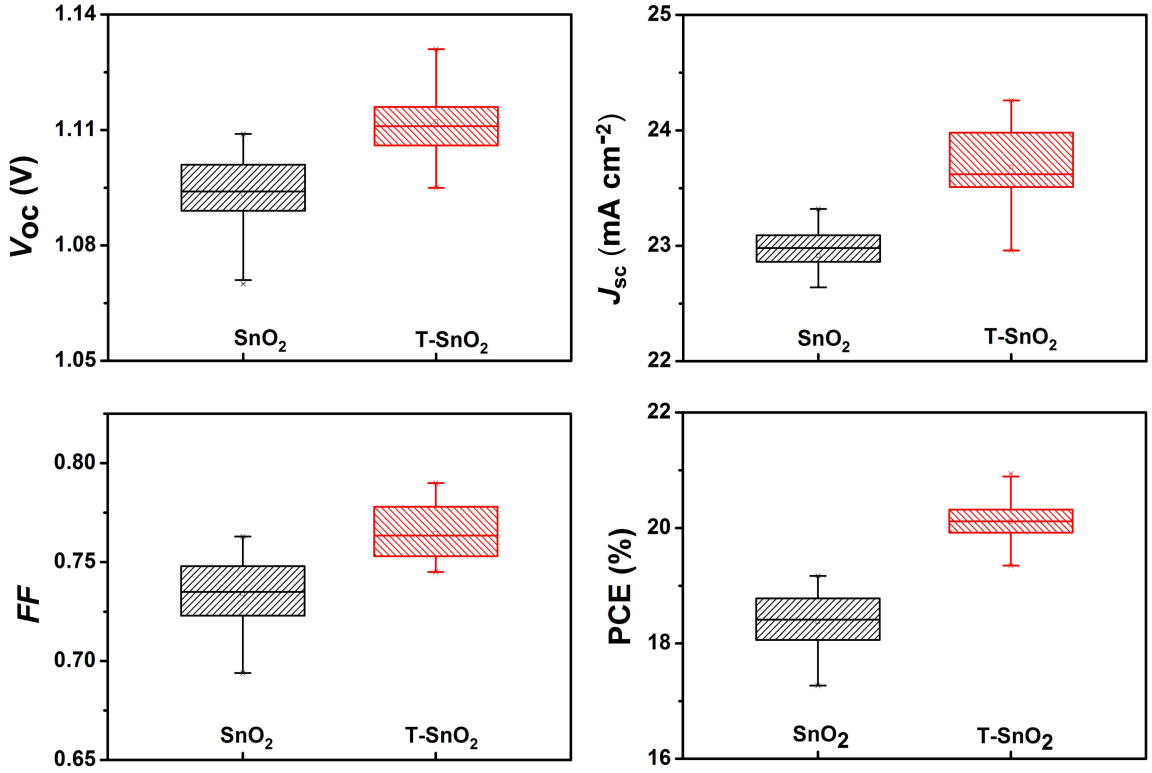


**Figure S10** Comparison of photovoltaic parameters for the $SnO_2$ and T-$SnO_2$ devices. There were 50 cells for each counted from 10 different batches. All the data are from reverse scan. Related to figure 2C.

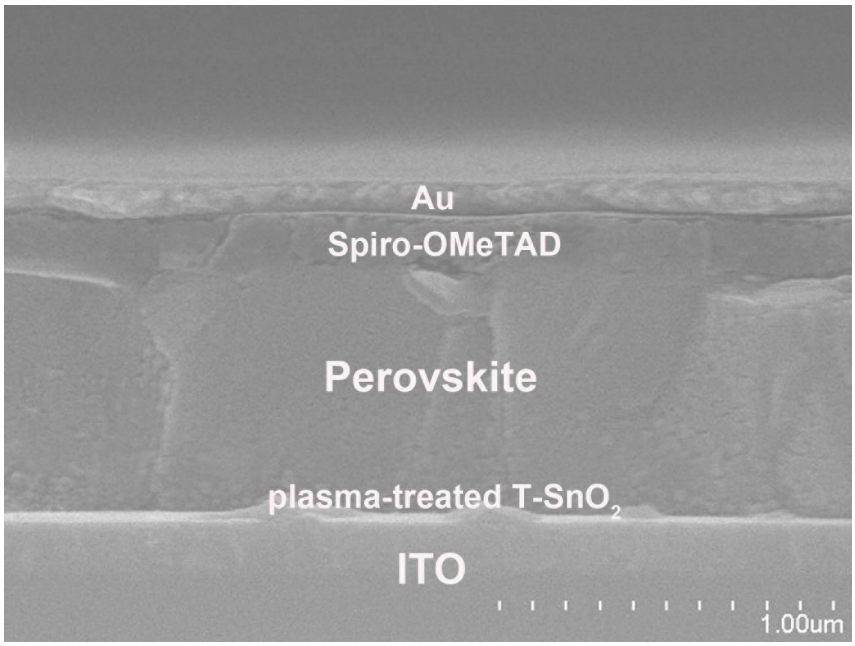


**Figure S11** SEM cross-sectional image of the p-T-$SnO_2$ device. Related to figure 4A.

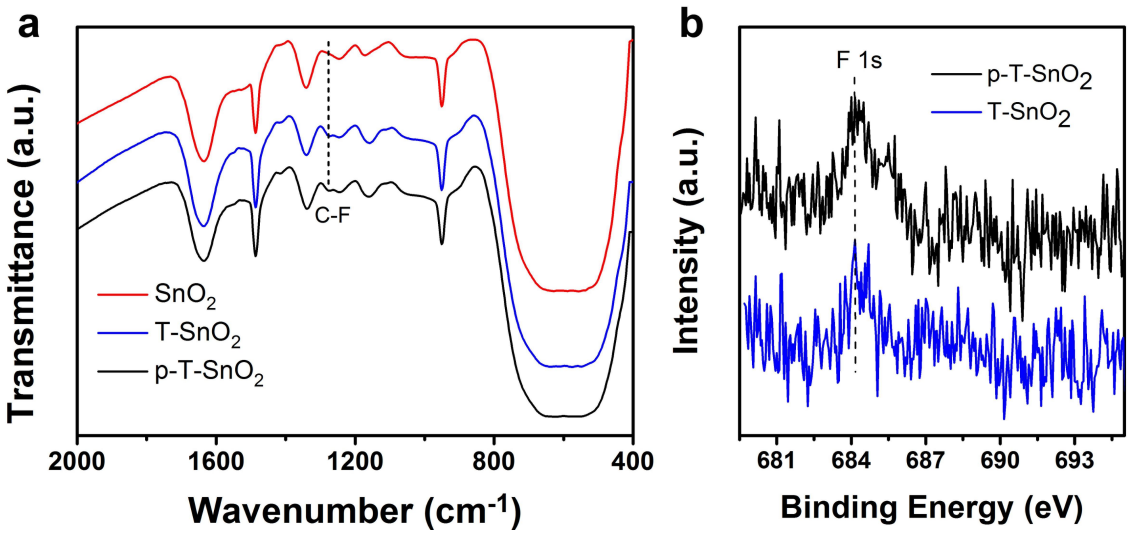


**Figure S12** a) FTIR spectra of the $SnO_2$, T-$SnO_2$ and p-T-$SnO_2$ films. b) XPS spectra of the F 1s peaks for the T-$SnO_2$ and p-T-$SnO_2$ films. Related to figure 4.

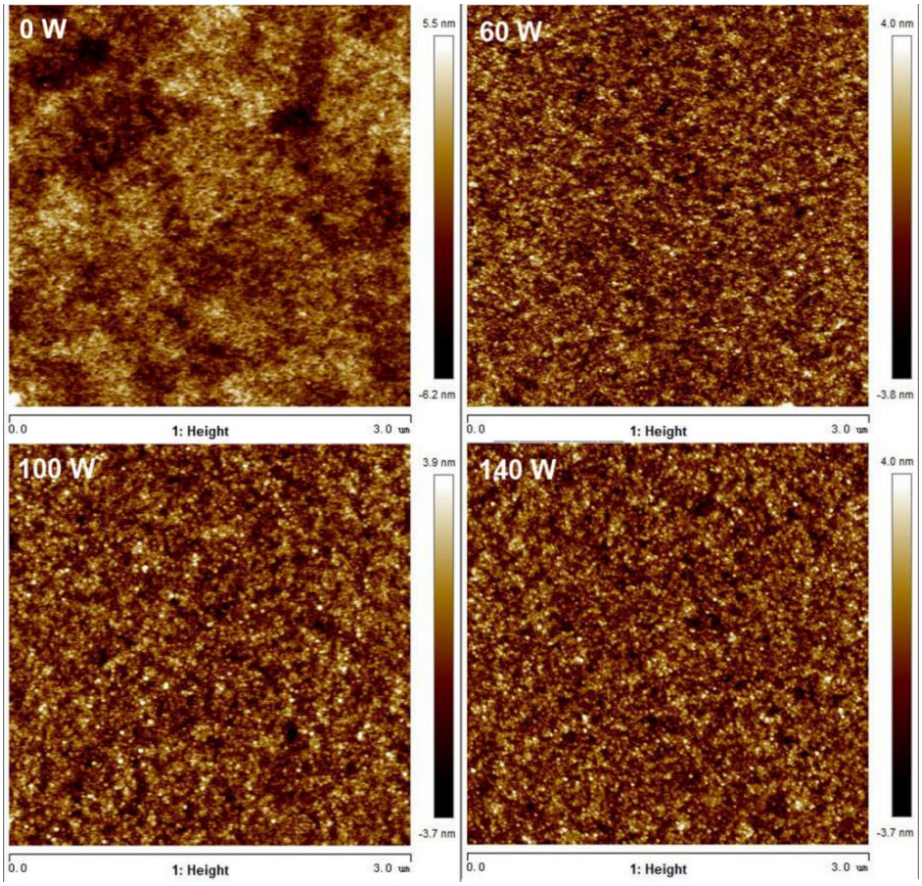


**Figure S13** The AFM images of the T-$SnO_2$ films (with different plasma powers). Note that the 0 W condition is T-$SnO_2$ without any plasma treated. Related to figure 4B.

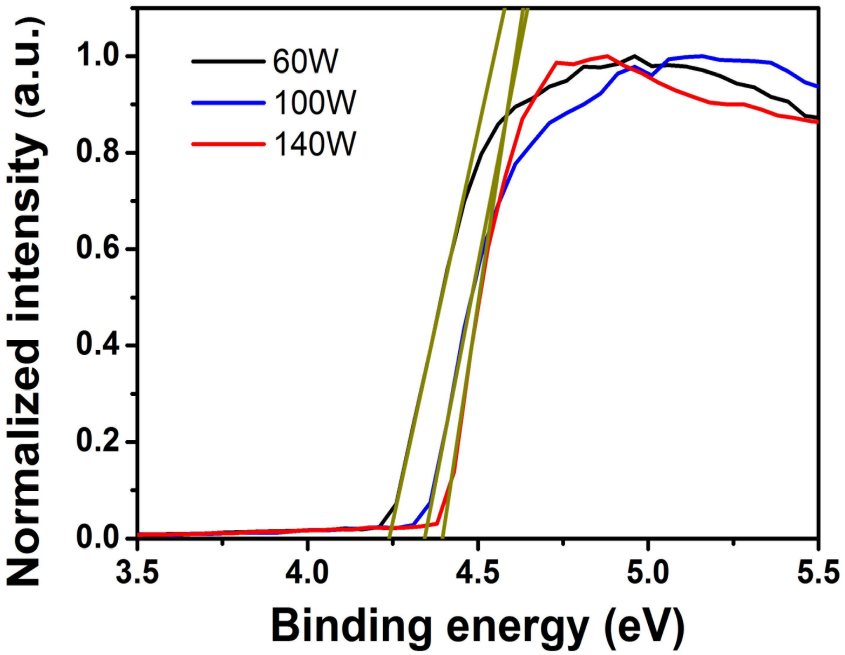


**Figure S14** The UPS cut-off edge of the T-$SnO_2$ films (with different plasma powers). Related to figure 4B.

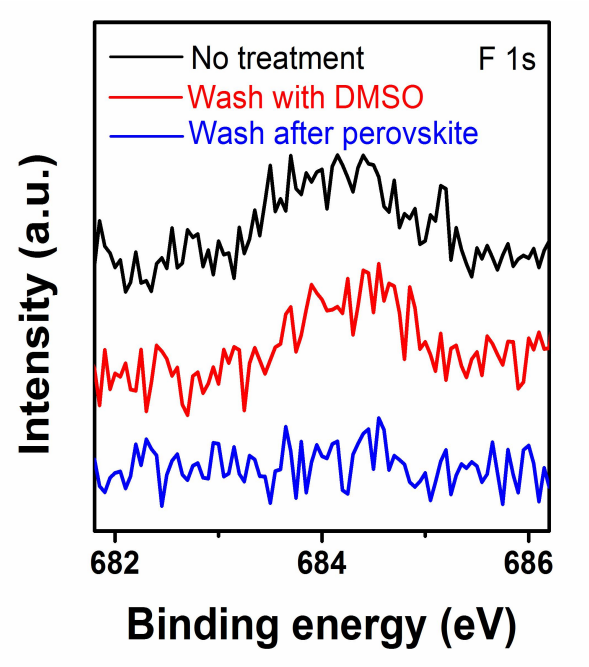


**Figure S15** The XPS spectra of F 1s peaks of T-$SnO_2$ films without any treatment, with DMSO washed and washed with DMSO after depositing perovskite on the T-$SnO_2$ films. and once fluorine entered into the perovskite lattice from the T-$SnO_2$/perovskite interface, it could be dissolved in DMSO. Related to figure 1A.

**Table S1** Photovoltaic parameters of the PSCs with different ETLs. Related to figure 2B.

| ETL | Scan direction | $V_{oc}$ (V) | $J_{sc}$ (mA cm$^{-2}$) | *FF* (-) | PCE (%) |
|---|---|---|---|---|---|
| $SnO_2$ | Reverse | 1.10 | 23.12 | 0.755 | 19.17 |
| | Forward | 1.06 | 23.03 | 0.674 | 16.47 |
| 100-T-$SnO_2$ | Reverse | 1.10 | 23.51 | 0.756 | 19.55 |
| | Forward | 1.06 | 23.43 | 0.703 | 17.49 |
| 250-T-$SnO_2$ | Reverse | 1.11 | 23.74 | 0.779 | 20.57 |
| | Forward | 1.08 | 23.69 | 0.757 | 19.33 |
| 350-T-$SnO_2$ | Reverse | 1.12 | 23.91 | 0.780 | 20.92 |
| | Forward | 1.11 | 23.87 | 0.777 | 20.62 |
| 380-T-$SnO_2$ | Reverse | 1.10 | 23.55 | 0.767 | 19.88 |
| | Forward | 1.09 | 23.54 | 0.766 | 19.71 |

**Table S2** Parameters of the TRPL spectra of perovskite deposited on different substrates. Related to figure 3C.

| Sample | $\tau_{ave}$/ns | $\tau_1$/ns | $A_1$ | $\tau_2$/ns | $A_2$ |
|---|---|---|---|---|---|
| Glass/perovskite | 763.36 | 303.56 | 41.68 | 890.16 | 51.54 |
| $SnO_2$/perovskite | 146.89 | 61.73 | 34.74 | 164.11 | 64.60 |
| T-$SnO_2$/perovskite | 52.39 | 10.65 | 35.60 | 56.64 | 65.74 |

**Table S3** EIS parameters of the $SnO_2$ and T-$SnO_2$ devices. Related to figure 3D.

| Substrates | $R_s$ (Ω) | $R_{tr}$ (Ω) | $C_{tr}$ (Ω) | $R_{rec}$ (Ω) | $C_{rec}$ (Ω) |
|---|---|---|---|---|---|
| **$SnO_2$** | 29.9 | 56.4 | 5.781E-8 | 294.2 | 1.056E-8 |
| **T-$SnO_2$** | 27.6 | 36.8 | 8.419E-8 | 650.5 | 4.480E-8 |

**Table S4** Photovoltaic parameters of the p-T-$SnO_2$ devices with different plasma powers at fixed $O_2$ gas flow rate of 0.05 L $h^{-1}$. Related to figure 4B.

| Style | Power (W) | $V_{oc}$ (V) | $J_{sc}$ (mA $cm^{-2}$) | *FF* (-) | PCE (%) |
|---|---|---|---|---|---|
| Oxygen plasma | 0 | 1.12 | 23.91 | 0.780 | 20.92 |
| | 60 | 1.12 | 24.06 | 0.802 | 21.68 |
| | 100 | 1.10 | 24.00 | 0.795 | 21.07 |
| | 140 | 1.07 | 23.92 | 0.796 | 20.35 |

**Table S5** Roughnesses of the p-T-$SnO_2$ films with different plasma powers at fixed $O_2$ gas flow rate of 0.05 L $h^{-1}$. The scan size of all the films is 3 um. The roughness is almost 32% lower than original one (pure T-SnO2), and when the power increased from 60 W to 140 W, the variation in roughness is negligible. Related to figure 4.

| Plasma power (W) | $R_q$ (nm) | $R_a$ (nm) | $R_{max}$ (nm) |
|---|---|---|---|
| 0 W | 1.67 | 1.27 | 14.2 |
| 60w | 1.13 | 0.89 | 12.1 |
| 100W | 1.09 | 0.86 | 12.6 |
| 160W | 1.08 | 0.86 | 11.2 |

**Table S6** Work functions of the p-T-$SnO_2$ films with different plasma powers at fixed $O_2$ gas flow rate of 0.05 L $h^{-1}$. Related to figure 4.

| Plasma power (W) | 0 | 60 | 100 | 140 |
|---|---|---|---|---|
| Work function (eV) | 4.19 | 4.21 | 4.34 | 4.40 |

## Transparent Methods

### Precursor $SnO_2$ and T-$SnO_2$ Solution

The $SnO_2$ precursor solution was obtained by diluting the $SnO_2$ colloidal solution (the concentration is 2.67%). For T-$SnO_2$ solution, the 2,2,2-Trifluoroethanol (aladdin) was added into the distilled water and fully stirred (the total volume is 650 μl). After that, the $SnO_2$ colloidal solution (100 μl) was added into the mixed solution. The solution was then heated to 32°C and stirred about 30 min to form T-$SnO_2$ solution.

### Fabrication of Solar Cells

The glass/ITO was washed in the order of cleanser essence, distilled water, acetone and isopropyl alcohol for 30 min. For the $SnO_2$ ETL, the precursor solution was spin-coated onto the ITO at 3500 rpm for 35 s, and then annealed at 150 °C for 30 min. For the T-$SnO_2$ ETL, the precursor solution was spin-coated onto the ITO at 3500 rpm for 35 s, and then annealed at 130 °C for 30 min. For the p-T-$SnO_2$ ETL, the T-$SnO_2$ ETL surface was treated by $O_2$ plasma for 5 min with various powers at a fixed $O_2$ flow rate of 0.05 L $h^{-1}$. The perovskite film was made by two-step method. For the first step, 760 mg $PbI_2$ was added into 1 ml DMF and 160 μl DMSO mixed solution, then was stirred over night at 25°C. The as-prepared solution was used as $PbI_2$ layer by spin-coating at 1600 rpm for 23 s and then 4000 rpm for 27 s, Then annealed at 70°C for 2 min. For the second step, the FAI: MACl: MABr mixed solution (110: 11: 11.5 mg in 1.5 ml isopropyl alcohol) was spin-coated onto the $PbI_2$ layer at 2000 rpm for 23 s, then the sample was taken out of the glove box and annealed at 140 °C for 20 min (ambient air,~ 40% humidity). After annealing, the sample was rapidly transferred to the glove box for HTL coating. The Spiro-OMeTAD (72.3 mg) in chlorobenzene (CB) solution (1 ml), adding 17.5 μl Li-TFSI/acetonitrile mixed solution (170 mg $ml^{-1}$) and 28.8 μl 4-tBP, which was coated at 4000 rpm for 27 s. After that, the sample was stored in the drying cabinet (ambient air, ~1% humidity) for 20 h. Finally, 90 nm Au electrode was deposited by vacuum evaporation at the pressure of $3\times10^{-6}$ Torr.

### Thin Film Characterization

UPS and XPS tests were performed on XPS machine (ESCALAB250XI, Thermo Fisher Scientific). The XRD patterns were obtained to research the crystallographic characteristics of perovskite, which was measured by using Rigaku-2500 X-ray diffractometer with CuKα radiation, λ =1.5406 Å. The surface morphology and cross section of the devices are investigated by SEM (S-4800, Japan). The surface roughness of the electron transfer layers were obtained by using atomic force microscope (AFM, Bruker MultiMode 8 SPM system).

### Electron Mobility Calculation

The electron mobilities of $SnO_2$ and T-$SnO_2$ films were calculated by the SCLC method. The Equation is below:

$$J = \frac{9}{8}\mu_e \varepsilon_0 \varepsilon_r \frac{V^2}{L^3}$$

Where $\mu_e$, $\varepsilon_0$, $\varepsilon_r$ and L are electron mobility, free space permittivity, dielectric constant and the thickness of electron transport layer.

### Average Carrier Lifetime Calculation

The carrier lifetime ($\tau_{ave}$) can be calculated using the Equation:

$$\tau_{ave} = \frac{\sum A_i \tau_i^2}{\sum A_i \tau_i}$$

where $A_i$ *and* $\tau_i$ are the decay amplitude and decay time.

**Device Characterization**

All *J-V* curves were measured using the Keithley 2420, and the solar cell was illuminated by a solar simulator (Newport 94043A, AM 1.5G, USA). The light intensity was calibrated by the monocrystalline silicon reference cell with a standard value 100 mW $cm^{-2}$. The device area was 0.044 $cm^2$. The external quantum efficiency (EQE) spectra was obtained with Newport 300 W Xenon Light Source (Newport IQE 200, USA). The electrical impedance spectroscopy (EIS) was measured by Zennium (Zahner).